Cubic contributions to the spherical model of shallow acceptor states

A. Baldereschi*
Bell Laboratories, Murray Hill, New Jersey 07974

Nunzio O. Lipari
Xerox Research Laboratories, Rochester, New York 14644

(Received 7 September 1973)

In a previous paper the effective-mass Hamiltonian for shallow acceptor states was separated into a spherical term and a cubic contribution. Neglecting the latter term, a spherical model was formulated which explained the main features of the experimental acceptor spectra. Here the effects of the cubic term are studied using perturbation theory, and all the details of the observed spectra are reproduced. As in the case of the spherical model, the eigenvalue problem is reduced to simple radial Hamiltonians which are explicitly given for the most important acceptor states. These Hamiltonians are solved numerically and the resulting eigenvalues are tabulated as functions of the relevant parameters. The predicted spectra are in good agreement with available experimental data for acceptors in Ge, InSb, and GaAs, but not for acceptors in Si, where the unusual strength of the cubic term makes the present analysis unsatisfactory.

I. INTRODUCTION

Recently we have formulated a new approach[1-3] to the problem of shallow acceptor states in semiconductors. In this formulation the acceptor Hamiltonian is separated into terms which have strict cubic symmetry and terms which, besides having cubic symmetry, are also spherically invariant. Since the former terms generally contribute to binding less than the latter, the cubic contribution can be neglected in first approximation and a spherical model of the acceptor system is obtained. In this model, the acceptor center is strongly similar to an atomic system with spin-orbit coupling, where different valence bands in the impurity case correspond to different spin states in the atomic counterpart. This approach has several advantages over previous investigations by other authors[4-9]: Among these are the simple formulation, which makes possible a clear insight of the acceptor problem, and the strong similarity to atomic systems, which allows the use of theorems and techniques of angular-momentum theory.

Although the spherical model, as it is, is satisfactory in explaining the general features of the experimental acceptor spectra, a more realistic model, which includes the cubic term in the Hamiltonian, is necessary to explain the details of the experimental data. In fact, the observed acceptor spectra exhibit a number of lines larger than that predicted by the spherical model. The cubic term, when added to the spherical model, produces shifts of the acceptor energy levels and, owing to its lower symmetry, introduces splittings of some degenerate states. The resulting theoretical spectrum has now all the features shown in the experimental data.

In the effective-mass acceptor Hamiltonian, the cubic contribution is generally small relative to the spherical term, and therefore can be treated in a perturbative scheme. The radial Hamiltonians describing the most important acceptor states in the spherical model are modified in order to include the effect of the additional cubic term using first-order perturbation theory in the limits of strong and weak spin-orbit coupling. These Hamiltonians are solved numerically using the variational method. The energy shifts and splittings thus obtained are expected to be accurate, except when the cubic contribution is strong. This means that the present treatment is generally valid for the investigation of acceptor states in diamond and zinc blende semiconductors, except for very few cases, like Si, where the cubic term is unusually large.

In Sec. II we outline the main aspects of the spherical model and analyze the modifications produced by the additional cubic terms in the limits of strong and weak spin-orbit coupling. In Sec. III we explicitly give the radial Hamiltonians describing the most important acceptor states and including the lowest-order couplings produced by the cubic term. In Sec. IV we solve numerically the various acceptor Hamiltonians and we tabulate the energy levels as functions of the relevant parameters. The theoretical acceptor spectrum is given for several diamond and zinc blende semiconductors and compared with available experimental data. In Sec. V we summarize the present work and discuss possible extensions. For convenience, we give in the Appendix the theorems on angular momentum which are used in the present paper.

II. CUBIC MODIFICATIONS TO SPHERICAL MODEL

In the effective-mass approximation, the acceptor Hamiltonian is[10]

$$H = (\gamma_1 + \tfrac{5}{2}\gamma_2)(p_2/2m_0) - (\gamma_2/m_0)(p_x^2 J_x^2 + p_y^2 J_y^2 + p_z^2 J_z^2) - (2\gamma_3/m_0)(\{p_x p_y\}\{J_x J_y\} + \{p_y p_z\}\{J_y J_z\} + \{p_z p_x\}\{J_z J_x\}) - (e^2/\epsilon_0 r) , \quad (1)$$

where $\{ab\} = \frac{1}{2}(ab + ba)$; ϵ_0 and m_0 are the crystal dielectric constant and the free-electron mass, respectively; γ_1, γ_2, and γ_3 are the Luttinger parameters which describe the hole dispersion relation near the center of the Brillouin zone; $\vec{p}$ is the hole linear-momentum operator, and $\vec{J}$ is the angular-momentum operator corresponding to spin $\frac{3}{2}$. Hamiltonian (1) is valid for diamond crystals in the limit of strong spin-orbit coupling in the valence bands, assuming that the acceptor center is described by a Coulomb potential screened by the static dielectric constant.

Following the same procedure used in our previous paper,[3] we introduce the second-rank Cartesian tensor operators

$$P_{ik} = 3 p_i p_k - \delta_{ik} p^2 \quad (2a)$$

and

$$J_{ik} = \tfrac{3}{2}(J_i J_k + J_k J_i) - \delta_{ik} J^2 \quad (2b)$$

and the corresponding irreducible components $P_q^{(2)}$ and $J_q^{(2)}$ $(q = -2, -1, 0, 1, 2)$. Using the effective rydberg

$$R_0 = e^4 m_0/2\hbar^2 \epsilon_0^2 \gamma_1 \quad (3a)$$

and the effective Bohr radius

$$a_0 = \hbar^2 \epsilon_0 \gamma_1/e^2 m_0 \quad (3b)$$

as units of energy and length, respectively; Hamiltonian (1) can be written as

$$H = (\hbar^2)^{-1} p^2 - \frac{2}{r} - (9\hbar^2)^{-1} \mu (P^{(2)} \cdot J^{(2)}) + (9\hbar^2)^{-1} \delta([P^{(2)} \times J^{(2)}]_4^{(4)} + \tfrac{1}{5}\sqrt{70}[P^{(2} \times J^{(2)}]_0^{(4)} + [P^{(2)} \times J^{(2)}]_{-4}^{(4)}) , \quad (4)$$

where, instead of the Luttinger valence-band parameters γ_1, γ_2, and γ_3, we use the spherical coupling parameter

$$\mu = (6\gamma_3 + 4\gamma_2)/5\gamma_1 , \quad (5)$$

which describes the strength of the spherical "spin-orbit" interaction, and the cubic coupling parameter

$$\delta = (\gamma_3 - \gamma_2)/\gamma_1 , \quad (6)$$

which measures the strength of the cubic contributions.

The spherical model[3] consists in neglecting the term in δ in Hamiltonian (4). With this assumption the acceptor Hamiltonian reduces to that of an hydrogen atom [the first two terms in (4)] modified by a spherical "spin-orbit" term whose strength is given by the parameter μ. The total angular momentum $\vec{F} = \vec{L} + \vec{J}$ is a constant of motion in this model, and the eigenstates can be classified according to the well-known L-S coupling scheme. For practical purposes, the most important acceptor levels are, neglecting the "spin-orbit" coupling, the hydrogenic S and P states. Including "spin-orbit" and using the L-S coupling scheme, the S states give rise only to $S_{3/2}$ states, whereas the P states split into $P_{1/2}$, $P_{3/2}$, and $P_{5/2}$. The energies of these levels can be obtained using the spherical-model Hamiltonians as described in our previous work.[3]

The cubic term in Hamiltonian (4) lowers the symmetry of the problem to that of the point group O_h,[11] and therefore the acceptor states must be classified according to the irreducible representations of this point group. The $S_{3/2}$ states transform like Γ_8^+, and therefore they shift in energy but do not split in the presence of the cubic term. The same occurs for $P_{1/2}$ and $P_{3/2}$ states, which transform like Γ_6^- and Γ_8^-, respectively. The $P_{5/2}$ states, instead, split into a twofold Γ_7^- and a fourfold Γ_8^- state.

In the spherical model, the acceptor energy spectrum shows a characteristic divergence in the binding energy for $\mu = 1$. This divergence was shown to be due to the fact that, for this value of the spherical coupling parameter μ, the upper valence band becomes flat. This peculiar behavior occurs for different values of the parameter μ when we take into account in Hamiltonian (4) the cubic term. In fact the valence-band energy dispersion is given by

$$E_\pm = -(\hbar^2\gamma_1/2m_0)\{k^2 \pm [(\mu - \tfrac{6}{5}\delta)^2 k^4 + \tfrac{12}{5}\delta(5\mu - \delta) \times (k_x^2 k_y^2 + k_y^2 k_z^2 + k_z^2 k_x^2)]^{1/2}\} , \quad (7)$$

which represents two parabolic bands whose curvature depends on the direction in k space. The smallest curvature is in the (1, 1, 1) direction, where the upper valence band has the following dispersion relation:

$$E_- = -(\hbar^2\gamma_1/2m_0)(1 - \mu - \tfrac{4}{5}\delta) k^2 . \quad (8)$$

Therefore for $\mu + \frac{4}{5}\delta = 1$ the upper valence band becomes flat in the $\langle 1, 1, 1\rangle$ and equivalent directions and the binding energy of all the acceptor states associated with this band will diverge.

We now study the acceptor problem in the opposite limiting case, i.e., the case of vanishing spin-orbit coupling in the valence bands. In this limit the acceptor Hamiltonian corresponding to

(4) is given by[3]

$$H' = (\hbar^2)^{-1} p^2 - \frac{2}{r} - (3\hbar^2)^{-1}(P^{(2)} \cdot I^{(2)}) + (3\hbar^2)^{-1}\delta([P^{(2)} \times I^{(2)}]_4^{(4)} + \tfrac{1}{5}\sqrt{70}[P^{(2)} \times I^{(2)}]_0^{(4)} + [P^{(2)} \times I^{(2)}]_{-4}^{(4)}, \quad (9)$$

where I is the angular-momentum operator corresponding to spin 1. Hamiltonian (9) is very similar to (4) except for the integer spin operator. In the spherical model ($\delta = 0$) we again use the L-S coupling scheme for the classification of the acceptor states. The hydrogenic S states give rise only to S_1 states, while the hydrogenic P states split into P_0, P_1, and P_2 states. Including the cubic term, the symmetry of (3) lowers to that of the point group O_h. The states S_1 transform like the irreducible representations Γ_{25}' and therefore they do not split. The same happens for P_0 and P_1 states, which transform like Γ_2' and Γ_{15}, respectively. The P_2 states, instead, split into Γ_{12}' and Γ_{25}. As in the strong spin-orbit case, the cubic term affects the values of the valence-band parameters for which a divergence occurs in the energy spectrum. In this case, the smallest curvature in the valence bands occurs in the (1, 1, 0) direction, where the upper valence band has the dispersion relation

$$E' = (-\hbar^2\gamma_1/2m_0)(1 - \mu - \tfrac{9}{5}\delta)\,k^2, \quad (10)$$

and therefore the divergence will now occur when $(\mu + \frac{9}{5}\delta) = 1$. This result shows that, for given μ and δ, the effect of the cubic term is stronger in the weak spin-orbit limit.

III. ANALYSIS OF CUBIC TERMS

A detailed study of the spherical-model Hamiltonian has been given in our previous work[3] in the limits of strong and weak spin-orbit coupling. In this model it was shown that the eigenvalue problem reduces to a simple radial Hamiltonian for each possible symmetry of the acceptor states. This was possible because in the spherical model the total angular momentum F is a good quantum number and the spherical "spin-orbit" term couples at most two different orbital angular momenta L. As a consequence, the radial Hamiltonians for the various acceptor states were at most 2×2 radial-operator matrices.

In the presence of the cubic "spin-orbit" term, the total angular momentum F is no longer a good quantum number, and all orbital angular momenta L of a given parity are coupled together. Therefore the order of the exact radial-operator matrices is infinite and their solution is practically impossible. In order to find solutions of the acceptor problem, it is necessary to reduce the above radial-operator matrices to a finite size. To this end we consider the values of the valence-band parameters for various diamond and zinc blende semiconductors, which are given in Table I. The cubic-coupling parameter δ is generally rather small compared to the spherical-coupling parameter μ. This fact is better shown in Fig. 1, which represents the valence-band energy dispersion relation of Ge and GaAs. In these materials the acceptor binding energy is of order $0.01 \sim 0.03$ eV, and we see that up to this energy the actual valence-band dispersion (i.e., including the cubic term) does not differ appreciably from the spherical model dispersion, which is obtained neglecting the cubic term. For diamond and zinc blende materials, therefore, it seems possible to treat the cubic term in Hamiltonians (4) and (9) as a perturbation on the spherical-model Hamiltonian. Among the substances listed in Table I, Si is the only material for which the above considerations do not apply, since $\delta/\mu = 0.5$. The valence-band dispersion of Si near the center of the Brillouin zone is shown in Fig. 2 together with that of GaP for reference. In the case of Si the strength of the cubic term is anomalously large, and the spherical-model dispersion is a poor representation of the actual band structure. Therefore we see that, with the only exception of Si, we can study the effects of the cubic term in the acceptor problem using first-order perturbation theory. With this approximation, the radial-operator matrices will be reduced to finite size and a solution of the acceptor problem will be possible. Since the effects produced by the cubic term are different for states with integer and semi-integer spin, we consider separately the cases of strong and weak spin-orbit coupling in the valence band.

A. Strong spin-orbit coupling

As in our previous work[3] we consider only the acceptor states $S_{3/2}$, $P_{1/2}$, $P_{3/2}$, and $P_{5/2}$. Only the $P_{5/2}$ states are affected by first-order cubic coupling. In the spherical model these states have the following wave function[3]:

$$\Phi(P_{5/2}) = f_3(r)\,|L=1,\ J=\tfrac{3}{2},\ F=\tfrac{5}{2},\ F_z\rangle + g_3(r)\,|L=3,\ J=\tfrac{3}{2},\ F=\tfrac{5}{2},\ F_z\rangle, \quad (11)$$

and the cubic term couples states that have $\Delta F_z = 0, \pm 4$. The coupling radial operators can be obtained using the "reduced-matrix-element" technique,[12] which in our particular case can be written as

$$\langle L', J, F, F_z'|\,[P^{(2)}\times J^{(2)}]_m^{(4)}\,|L, J, F, F_z\rangle = 3\times(-1)^{F-F_z'}(2F+1)\begin{pmatrix} F & 4 & F \\ -F_z' & m & F_z\end{pmatrix} \times \begin{Bmatrix} J & J & 2 \\ L' & L & 2 \\ F & F & 4\end{Bmatrix}(J\|J^{(2)}\|J)(L'\|P^{(2)}\|L), \quad (12)$$

TABLE I. Values of the static dielectric constant ϵ_0 and of the valence-band parameters γ_1, γ_2, and γ_3 used in the present calculation. The valence-band parameters μ and δ introduced in connection with the spherical model are also given together with the energy and length units R_0 and a_0, respectively.

	ϵ_0	γ_1 [a]	γ_2 [a]	γ_3 [a]	μ	δ	R_0 (MeV)	a_0(Å)
Si	11.40[b]	4.22	0.39	1.44	0.483	0.249	24.8	25.5
Ge	15.36[b]	13.35	4.25	5.69	0.766	0.108	4.3	108.5
AlSb	12.0[c]	4.15	1.01	1.75	0.701	0.178	22.8	26.4
GaP	10.75[d]	4.20	0.98	1.66	0.661	0.162	28.0	23.9
GaAs	12.56[e]	7.65	2.41	3.28	0.767	0.114	11.3	50.8
GaSb	15.7[c]	11.80	4.03	5.26	0.808	0.104	4.7	98.0
InP	12.4[f]	6.28	2.08	2.76	0.792	0.108	14.1	41.2
InAs	14.6[g]	19.67	8.37	9.29	0.907	0.047	3.2	152.0
InSb	17.9[c]	35.08	15.64	16.91	0.935	0.036	1.2	332.3
ZnS	8.1[h]	2.54	0.75	1.09	0.751	0.134	81.6	10.9
ZnSe	9.1[h]	3.77	1.24	1.67	0.795	0.114	43.6	18.2
ZnTe	10.1[h]	3.74	1.07	1.64	0.755	0.152	35.7	20.0
CdTe	9.7[h]	5.29	1.89	2.46	0.844	0.108	27.3	27.2

[a]For valence-band parameters see P. Lawaetz, Phys. Rev. B 4, 3460 (1971).
[b]R. A. Faulkner, Phys. Rev. 184, 713 (1969).
[c]M. Hass and B. W. Henvis, J. Phys. Chem. Solids 23, 1099 (1962).
[d]L. Patrick and P. J. Dean, Phys. Rev. 188, 1254 (1969).
[e]G. E. Stillman, D. M. Larsen, C. M. Wolfe, and R. C. Brandt, Solid State Commun. 9, 2245 (1971).
[f]C. Hilsum, S. Fray, and C. Smith, Solid State Commun. 7, 1057 (1969).
[g]O. G. Lorimor and W. G. Spitzer, J. Appl. Phys. 36, 1841 (1965).
[h]D. Berlincourt, H. Jaffe, and L. R. Shiozawa, Phys. Rev. 129, 1009 (1963).

where the reduced matrix elements $(J \| J^{(2)} \| J)$ and $(L' \| P^{(2)} \| L)$ are explicitly given in our previous work[3]; the values of the 6-j symbol can be found in Rotemberg *et al.*,[13] and the values of the 9-j symbol needed in the present work are explicitly given in the Appendix.

As a result of the cubic coupling between the spherical-model states (11) with different F_z, the $P_{5/2}$ states split into a Γ_7^- and Γ_8^- state whose wave functions can be represented as

$$\Phi(P_{5/2},\ \Gamma_7^-) = f_3'(r)\,|\,L=1,\ J=\tfrac{3}{2},\ F=\tfrac{5}{2},\ \Gamma_7^-\rangle + g_3'(r)\,|\,L=3,\ J=\tfrac{3}{2},\ F=\tfrac{5}{2},\ \Gamma_7^-\rangle \quad (13a)$$

and

$$\Phi(P_{5/2},\ \Gamma_8^-) = f_3''(r)\,|\,L=1,\ J=\tfrac{3}{2},\ F=\tfrac{5}{2},\ \Gamma_8^-\rangle + g_3''(r)\,|\,L=3,\ J=\tfrac{3}{2},\ F=\tfrac{5}{2},\ \Gamma_8^-\rangle\,, \quad (13b)$$

where the symbols Γ_7^- and Γ_8^-, which appear on the right-hand side, indicate the appropriate linear combination of states with different component F_z of the total angular momentum which transform according to the given irreducible representation of the point group O_h. Adding the cubic contributions (12) to the $P_{5/2}$ spherical-model Hamiltonian, we obtain the following radial Hamiltonian for the $P_{5/2}(\Gamma_7^-)$ states:

$$\begin{vmatrix} \left(1+\frac{1}{5}\mu+\frac{24}{25}\delta\right)\left(\frac{d^2}{dr^2}+\frac{2}{r}\frac{d}{dr}-\frac{2}{r^2}\right)+\frac{2}{r}-E & -\frac{2\sqrt{6}}{5}\left(\mu-\frac{1}{5}\delta\right)\left(\frac{d^2}{dr^2}+\frac{7}{r}\frac{d}{dr}+\frac{8}{r^2}\right) \\ -\frac{2\sqrt{6}}{5}\left(\mu-\frac{1}{5}\delta\right)\left(\frac{d^2}{dr^2}-\frac{3}{r}\frac{d}{dr}+\frac{3}{r^2}\right) & \left(1-\frac{1}{5}\mu-\frac{68}{175}\delta\right)\left(\frac{d^2}{dr^2}+\frac{2}{r}\frac{d}{dr}-\frac{12}{r^2}\right)+\frac{2}{r}-E \end{vmatrix} \cdot \begin{vmatrix} f_3'(r) \\ g_3'(r) \end{vmatrix} = 0, \quad (14a)$$

and the following Hamiltonian for the $P_{5/2}(\Gamma_8^-)$ states

$$\begin{vmatrix} \left(1+\frac{1}{5}\mu-\frac{12}{25}\delta\right)\left(\frac{d^2}{dr^2}+\frac{2}{r}\frac{d}{dr}-\frac{2}{r^2}\right)+\frac{2}{r}-E & -\frac{\sqrt{6}}{5}\left(2\mu+\frac{1}{5}\delta\right)\left(\frac{d^2}{dr^2}+\frac{7}{r}\frac{d}{dr}+\frac{8}{r^2}\right) \\ -\frac{\sqrt{6}}{5}\left(2\mu+\frac{1}{5}\delta\right)\left(\frac{d^2}{dr^2}-\frac{3}{r}\frac{d}{dr}+\frac{3}{r^2}\right) & \left(1-\frac{1}{5}\mu+\frac{34}{115}\delta\right)\left(\frac{d^2}{dr^2}+\frac{2}{r}\frac{d}{dr}-\frac{12}{r^2}\right)+\frac{2}{r}-E \end{vmatrix} \cdot \begin{vmatrix} f_3''(r) \\ g_3''(r) \end{vmatrix} = 0\,. \quad (14b)$$

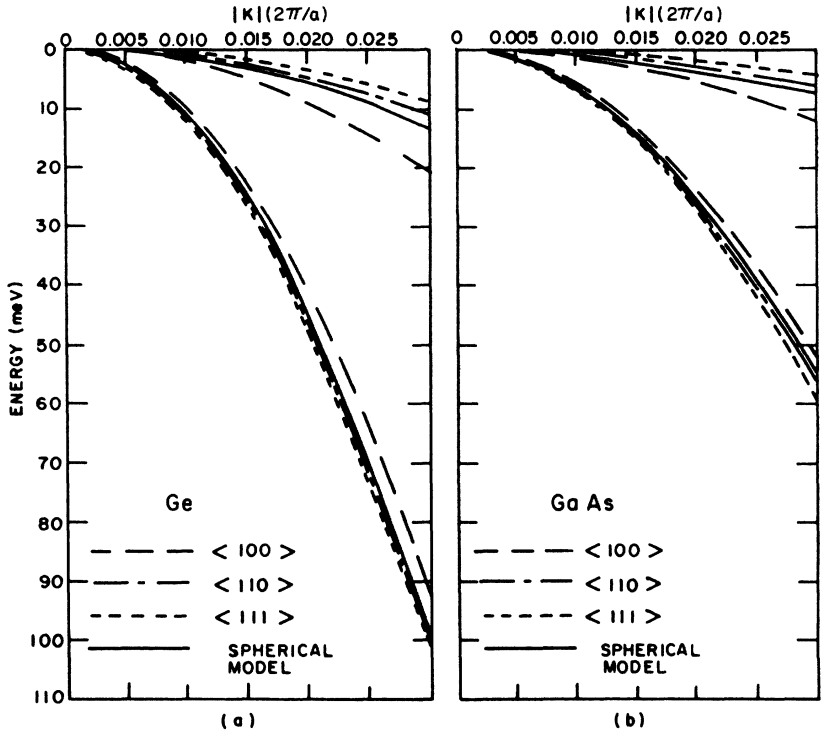

FIG. 1. Energy-dispersion relation for the valence bands of Ge and GaAs along the main symmetry directions. The deviations between the real valence bands and those predicted by the spherical model (also shown) are produced by the cubic term.

For $\delta = 0$ the above Hamiltonians reduce to the spherical-model Hamiltonian for $P_{5/2}$ states given in our previous work.[3]

A more accurate treatment of the cubic terms in the acceptor Hamiltonian requires the inclusion of couplings of order higher than the first. Even in second order, however, the problem becomes very complicated because of the infinite number of possible couplings. In order to have an idea of the contributions from higher-order effects, we consider the particularly important coupling between the $P_{5/2}(\Gamma_8^-)$ and $P_{3/2}(\Gamma_8^-)$ states, which are generally rather close in energy since they originate from the same unperturbed hydrogenic states. The cubic coupling between these two states can be obtained using the "reduced-matrix-element" technique, which in this case gives an expression for the matrix elements which is slightly different from (12), since the coupled states have different total angular momentum F. Using this more general expression, which is given in the Appendix, we obtain for the coupled $P_{5/2}(\Gamma_8^-)$ and $P_{3/2}(\Gamma_8^-)$ states the radial Hamiltonian

$$H_c = \begin{vmatrix} H(\tfrac{3}{2}) & \sqrt{6}\,X \\ \sqrt{6}\,X^{+} & H(\tfrac{5}{2}, \Gamma_8^-) \end{vmatrix} , \tag{15}$$

where $H(\frac{5}{2}, \Gamma_8^-)$ is the Hamiltonian for $P_{5/2}(\Gamma_8^-)$ states given by (14b); $H(\frac{3}{2})$ is the Hamiltonian for $P_{3/2}$ states given by expression (27c) of our previous work[3]; and the coupling matrix X is

$$X = \begin{vmatrix} \frac{2\sqrt{6}}{25}\,\delta\left(\frac{d^2}{dr^2} + \frac{2}{r}\frac{d}{dr} - \frac{2}{r^2}\right) & -\frac{18}{175}\,\delta\left(\frac{d^2}{dr^2} + \frac{7}{r}\frac{d}{dr} + \frac{8}{r^2}\right) \\ -\frac{2\sqrt{6}}{175}\,\delta\left(\frac{d^2}{dr^2} - \frac{3}{r}\frac{d}{dr} + \frac{3}{r^2}\right) & \frac{22}{525}\,\delta\left(\frac{d^2}{dr^2} + \frac{2}{r}\frac{d}{dr} - \frac{12}{r^2}\right) \end{vmatrix} . \tag{16}$$

Hamiltonians (14a), (14b), and (15) cannot be solved exactly and their approximate solutions will be given in Sec. IV.

B. Weak spin-orbit coupling

Among the acceptor states S_1, P_0, P_1, and P_2, only P_2 states are affected by first-order cubic coupling. In the spherical model, the wave function for the P_2 states is[3]

$$\Phi(P_2) = F_3(r)\,|\,L=1,\ I=1,\ F=2,\ F_z\rangle + G_3(r)\,|\,L=3,\ I=1,\ F=2,\ F_z\rangle , \tag{17}$$

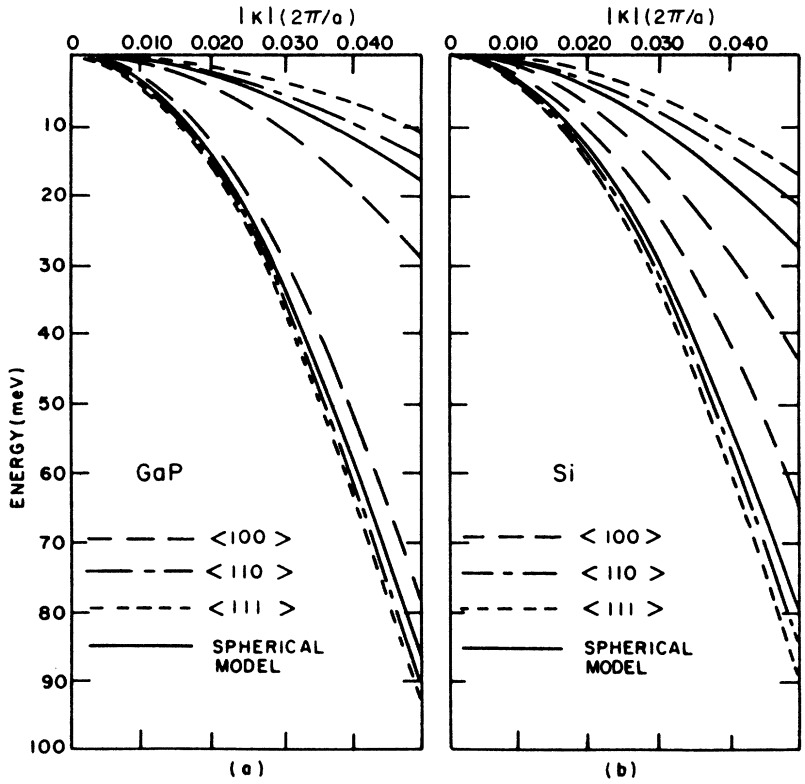

FIG. 2. Same as Fig. 1 but for the valence bands of GaP and Si. Note the dramatic effect produced by the cubic term in the case of Si.

and the cubic term couples states which have $\Delta F_z = 0, \pm 4$ and splits P_2 states into a twofold Γ_{12}' and a threefold Γ_{25} state. Using the reduced-matrix-element formula (12) and the unperturbed spherical-model Hamiltonian, we obtain the following radial Hamiltonian for the $P_2(\Gamma_{12}')$ states:

$$\begin{vmatrix} \left(1+\frac{1}{5}\mu-\frac{36}{25}\delta\right)\left(\frac{d^2}{dr^2}+\frac{2}{r}\frac{d}{dr}-\frac{2}{r^2}\right)+\frac{2}{r}-E & \frac{3\sqrt{6}}{5}\left(\mu+\frac{2}{35}\delta\right)\left(\frac{d^2}{dr^2}+\frac{7}{r}\frac{d}{dr}+\frac{8}{r^2}\right) \\ \frac{3\sqrt{6}}{5}\left(\mu+\frac{2}{35}\delta\right)\left(\frac{d^2}{dr^2}-\frac{3}{r}\frac{d}{dr}+\frac{3}{r^2}\right) & \left(1+\frac{4}{5}\mu-\frac{24}{525}\delta\right)\left(\frac{d^2}{dr^2}+\frac{2}{r}\frac{d}{dr}-\frac{12}{r^2}\right)+\frac{2}{r}-E \end{vmatrix} \begin{vmatrix} F_3'(r) \\ G_3'(r) \end{vmatrix} = 0, \tag{18a}$$

and the following Hamiltonian for the $P_2(\Gamma_{25})$ states:

$$\begin{vmatrix} \left(1+\frac{1}{5}\mu+\frac{24}{25}\delta\right)\left(\frac{d^2}{dr^2}+\frac{2}{r}\frac{d}{dr}-\frac{2}{r^2}\right)+\frac{2}{r}-E & \frac{\sqrt{6}}{5}\left(3\mu-\frac{4}{35}\delta\right)\left(\frac{d^2}{dr^2}+\frac{7}{r}\frac{d}{dr}+\frac{8}{r^2}\right) \\ \frac{\sqrt{6}}{5}\left(3\mu-\frac{4}{35}\delta\right)\left(\frac{d^2}{dr^2}-\frac{3}{r}\frac{d}{dr}+\frac{3}{r^2}\right) & \left(1+\frac{4}{5}\mu+\frac{16}{525}\delta\right)\left(\frac{d^2}{dr^2}+\frac{2}{r}\frac{d}{dr}-\frac{12}{r^2}\right)+\frac{2}{r}-E \end{vmatrix} \begin{vmatrix} F_3''(r) \\ G_3''(r) \end{vmatrix} = 0 . \tag{18b}$$

The above Hamiltonians will be numerically solved in Sec. IV.

IV. METHOD OF SOLUTION AND RESULTS

In Sec. III we have seen that the inclusion of the cubic term in the acceptor Hamiltonian affects, in the limit of first-order of perturbation theory, the state $P_{5/2}$ for strong spin-orbit coupling and the state P_2 for weak spin-orbit coupling. The resulting radial Hamiltonians (14a), (14b), (15), (18a), and (18b), which describe the above acceptor states in the presence of the cubic perturbation, cannot be solved exactly, and to find their eigenvalues and eigenfunctions we have used the variational technique along the same lines used in our previous work.[3] We have assumed as trial wave functions, superpositions of Gaussian func-

tions times the lowest possible polynomials which behave correctly at the origin. For the state $P_{5/2}(\Gamma_7^-)$ for example, which is described by Hamiltonian (14a), we have used as trial functions

$$f_3'(r) = r \sum_{i=1}^{21} A_i e^{-\alpha_i r^2} \tag{19a}$$

and

$$g_3'(r) = r^2 \sum_{i=1}^{21} B_i e^{-\alpha_i r^2} , \tag{19b}$$

where the linear parameters A_i and B_i were treated as variational parameters in order to minimize the energy, and throughout the calculations we used the same constant set of values for the 21 parameters α_i. The latter parameters have been chosen in geometrical progression ($\alpha_{i+1} = g\alpha_i$, with g independent of i) and their range of values is wide enough to cover all actual situations met in studying the acceptor spectrum, the smallest value being $\alpha_1 = 1\times10^{-2}$ and the largest $\alpha_{21} = 5\times10^{5}$.

The radial Hamiltonians (14b), (15), (18a), and (18b), which describe the remaining acceptor states studied in the present work, have been solved using trial functions of the form (19a) and (19b) with the same constant set of values for the 21 parameters α_i.

The energies of the lowest acceptor states of interest which are affected in first order of perturbation theory are tabulated as functions of the coupling parameters μ and δ in Tables II, III, and IV for the case of strong spin-orbit interaction.

TABLE II. Energy of the $2P_{5/2}(\Gamma_7^-)$ acceptor state as function of the coupling parameters μ and δ. The energy unit is the effective rydberg R_0.

μ \ δ	0.0	0.05	0.10	0.15	0.20	0.25
0.00	0.250	0.239	0.228	0.219	0.210	0.202
0.05	0.248	0.237	0.226	0.217	0.208	0.200
0.10	0.248	0.236	0.226	0.216	0.207	0.199
0.15	0.248	0.237	0.226	0.216	0.207	0.199
0.20	0.251	0.239	0.228	0.218	0.209	0.200
0.25	0.256	0.243	0.231	0.221	0.211	0.203
0.30	0.262	0.248	0.236	0.225	0.215	0.206
0.35	0.270	0.256	0.243	0.232	0.221	0.212
0.40	0.281	0.266	0.252	0.240	0.229	0.219
0.45	0.295	0.278	0.264	0.251	0.239	0.228
0.50	0.322	0.295	0.279	0.264	0.252	0.240
0.55	0.336	0.315	0.298	0.282	0.268	0.255
0.60	0.366	0.342	0.322	0.304	0.289	0.275
0.65	0.406	0.378	0.354	0.333	0.315	0.299
0.70	0.461	0.426	0.397	0.372	0.351	0.332
0.75	0.539	0.494	0.456	0.425	0.398	0.376
0.80	0.657	0.594	0.543	0.501	0.466	0.436
0.85	0.857	0.756	0.678	0.616	0.567	0.526
0.90	1.259	1.059	0.917	0.812	0.732	0.668
0.95	2.470	1.821	1.488	1.215	1.050	0.930
1.00	∞	7.199	3.667	2.493	1.909	1.561

TABLE III. Energy of the $2P_{3/2}(\Gamma_8^-)$ acceptor state as function of the coupling parameters μ and δ. The energy unit is the effective rydberg R_0.

μ \ δ	0.0	0.05	0.10	0.15	0.20	0.25
0.00	0.250	0.260	0.271	0.283	0.296	0.310
0.05	0.261	0.265	0.274	0.286	0.298	0.313
0.10	0.273	0.275	0.282	0.292	0.304	0.318
0.15	0.287	0.288	0.293	0.302	0.313	0.326
0.20	0.302	0.304	0.308	0.315	0.325	0.388
0.25	0.320	0.321	0.325	0.331	0.341	0.354
0.30	0.341	0.342	0.345	0.351	0.361	0.373
0.35	0.365	0.366	0.369	0.375	0.384	0.397
0.40	0.394	0.395	0.398	0.404	0.413	0.426
0.45	0.428	0.428	0.432	0.438	0.448	0.462
0.50	0.468	0.469	0.473	0.480	0.490	0.506
0.55	0.518	0.519	0.523	0.531	0.543	0.561
0.60	0.580	0.581	0.586	0.596	0.610	0.632
0.65	0.660	0.662	0.668	0.680	0.699	0.727
0.70	0.767	0.770	0.778	0.794	0.820	0.859
0.75	0.917	0.921	0.933	0.957	0.997	1.058
0.80	1.142	1.148	1.168	1.210	1.282	1.396
0.85	1.518	1.529	1.571	1.663	1.832	2.115
0.90	2.268	2.301	2.436	2.768	3.454	4.919
0.95	4.521	4.774	6.242	12.324	755.358	∞
1.00	∞	∞	∞	∞	∞	∞

The energies given in Table III and IV for the states $2P_{3/2}(\Gamma_8^-)$ and $2P_{5/2}(\Gamma_8^-)$ are the eigenvalues of the more general Hamiltonian (15), which takes into account the higher-order coupling between these two states. Neglecting such coupling, the above states are described by Hamiltonian (27c) of our previous work[3] and Hamiltonian (14b), respectively. The energies calculated with and without the above coupling are given in Table V for a few typical values of parameters μ and δ. The acceptor states $1S_{3/2}$, $2S_{3/2}$, and $2P_{1/2}$ are not affected in first order by the cubic term, and their energies calculated in the limit of the spherical model remain valid. For convenience we give the energies of these states in Table VI as functions of the coupling parameter μ, which is the only relevant parameter in this case. The acceptor energy spectrum as function of μ and for the typical value $\delta = 0.15$ is given in Figs. 3 and 4 in the cases of strong and weak spin-orbit coupling in the valence band, respectively. These figures show the peculiar effect of the cubic term on the acceptor spectrum, i.e., the cubic-term-induced splitting of the $P_{5/2}$ and P_2 states. The effect of the cubic term on the acceptor wave functions cannot be tabulated in simple form as function of the coupling parameters μ and δ. To give an idea of this effect, we compare in Figs. 5–7 the acceptor wave functions for $\delta = 0$ to those for $\delta = 0.15$ for the strong spin-orbit states $2P_{3/2}(\Gamma_8^-)$, $2P_{5/2}(\Gamma_8^-)$, and $2P_{5/2}(\Gamma_7^-)$, and for the

TABLE IV. Energy of the $2P_{5/2}(\Gamma_8^-)$ acceptor state as function of the coupling parameters μ and δ. The energy unit is the effective rydberg R_0.

μ \ δ	0.0	0.05	0.10	0.15	0.20	0.25
0.00	0.250	0.246	0.243	0.240	0.237	0.234
0.05	0.248	0.251	0.249	0.246	0.243	0.241
0.10	0.248	0.252	0.253	0.252	0.250	0.248
0.15	0.249	0.254	0.257	0.258	0.257	0.255
0.20	0.251	0.257	0.261	0.263	0.264	0.263
0.25	0.256	0.262	0.267	0.270	0.272	0.272
0.30	0.262	0.268	0.274	0.278	0.281	0.283
0.35	0.270	0.277	0.283	0.289	0.292	0.295
0.40	0.281	0.288	0.296	0.302	0.307	0.310
0.45	0.295	0.303	0.311	0.318	0.324	0.328
0.50	0.322	0.322	0.331	0.339	0.346	0.352
0.55	0.336	0.346	0.357	0.366	0.375	0.381
0.60	0.366	0.378	0.391	0.402	0.412	0.420
0.65	0.406	0.421	0.436	0.450	0.462	0.472
0.70	0.461	0.479	0.498	0.516	0.531	0.544
0.75	0.539	0.564	0.589	0.612	0.633	0.650
0.80	0.657	0.694	0.730	0.764	0.792	0.815
0.85	0.857	0.917	0.977	1.031	1.074	1.120
0.90	1.259	1.385	1.508	1.609	1.758	2.397
0.95	2.470	2.943	3.361	6.051	255.730	∞
1.00	∞	∞	∞	∞	∞	∞

values $\mu = 0.4$ and $\mu = 0.8$. Finally we give in Table VII the theoretically predicted acceptor energy levels for various diamond and zinc blende semiconductors. These values have been obtained using the valence-band parameters given in Table I and interpolating linearly on the energy Tables II–IV and VI. It should be noted that the above energy tables allow a straightforward calculation of the most important acceptor energy levels once the valence-band parameters of any given substance are known.

The theoretical energy levels obtained in the present work will now be compared with available experimental results. The most studied acceptor spectra are those in germanium and silicon, where several experimental works[14–16] have provided the transition energies from the ground state to various excited states. The acceptor ionization energies are known[17] for most of the III-V and II-VI compounds, but detailed excitation spectra are known only for acceptors in InSb[18] and in GaAs.[19]

The experimental excitation spectra for various acceptors and double acceptors in Ge are reproduced in Fig. 8, which clearly shows that all these spectra are very similar to each other except for the ground-state binding energy, which, owing to chemical effects, is different for different impurities. Since our theory does not take into account chemical shifts, we are not able to compare the absolute values of the excitation energies, and we will limit our considerations to line spacings. We expect the excitation spectrum to be dominated by optical transitions from the ground state to the hydrogenic $2P$ excited states, and we will show that this is indeed the case if we take into account the complicated structure of the valence bands, including also the cubic term. Because of the four-fold valence band (which can be thought of as a spin-$\frac{3}{2}$ particle), we have seen in the spherical-model that each one of the hydrogenic P states splits into three levels: $P_{1/2}$, $P_{3/2}$, and $P_{5/2}$. Furthermore, owing to the presence of the

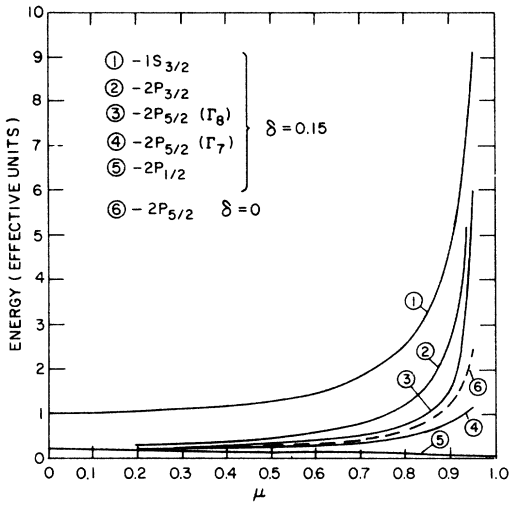

FIG. 3. Effect of the cubic term on the acceptor energy spectrum in the strong spin-orbit coupling limit. The typical value $\delta = 0.15$ has been assumed for the cubic coupling parameter. The energies are in units of the effective rydberg R_0.

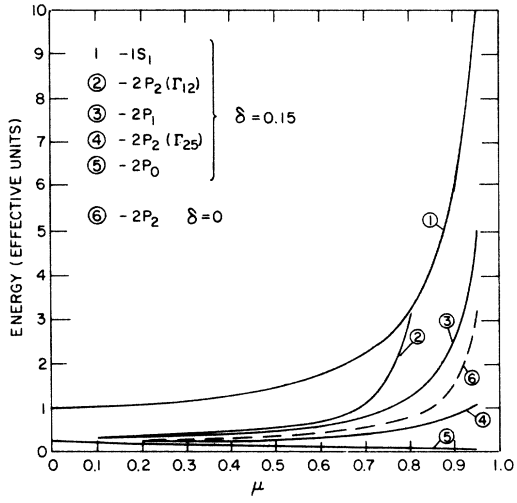

FIG. 4. Same as Fig. 3 but in the weak spin-orbit coupling limit.

cubic term, the $P_{5/2}$ states are split into the doublet $P_{5/2}(\Gamma_7^-)$ and $P_{5/2}(\Gamma_8^-)$.

The energies given in Table VII give us the order of the above levels and we can predict the following excitation spectrum for acceptors in Ge. The lowest energy transition is from the ground state to the $2P_{3/2}$ state, which theory predicts at an energy of 5.4 meV. This excitation peak should be followed by transitions to the $2P_{5/2}$ doublet, which should occur at 1.6 and 2.3 meV on the high-energy side of the $2P_{3/2}$ peak. The $2P_{5/2}(\Gamma_8^-)$ peak should occur at lower energy and the doublet splitting should be 0.7 meV. Transitions to the $2P_{1/2}$ states should occur at much higher energy, close to the series limit. Possibly transitions to the hydrogenic $3P$ states will occur (with the exception of $3P_{1/2}$) between the $2P_{5/2}$ doublet and $2P_{1/2}$. These qualitative features of the acceptor spectrum can indeed by seen in Fig. 8, where, together with the experimental results, we give by vertical broken lines the theoretical predictions. The experimental data show a prominent doublet, which both for the line spacing of 0.7 meV and the absolute energy position, is easily identified as the $2P_{5/2}$ doublet. We take the low-energy line of the doublet as the reference line. It is labeled line 3 in Fig. 8, and corresponds to transitions from the ground state to the $2P_{5/2}(\Gamma_8^-)$ state. The partner line of the doublet, line 4, corresponds to excitations to the $2P_{5/2}(\Gamma_7^-)$ state. The weaker line 1 on the low-energy side of the spectra is interpreted as being due to transitions to the $2P_{3/2}$ state, whereas the transitions to the highly excited $2P_{1/2}$ state, which should occur at the energy given by line 5, are not easily found in the experimental data, which, in this energy range, show a complicated and poorly resolved structure.

Since the acceptor P states are not expected to be affected by chemical effects—which occur only very close to the impurity site, where P functions have very small amplitude—the line spacings among the various excited P states should not be affected by chemical shifts, and therefore they should be well predicted by our theory. This is indeed the case, as can be seen from Fig. 8, or even better from Table VIII, which compares the theoretically predicted line spacings with the experimental data for various acceptors and double acceptors in Ge. On the high-energy side of the $2P_{5/2}$ doublet the experimental data in general show three more peaks which, in the literature, are labeled B, A', and A''. The peaks A' and A'' are very close in energy and strongly resemble a doublet. The energy spacings among those extra peaks do not show chemical effects and therefore suggest transitions to excited P states.

We can tentatively interpret the low-energy peak B as transitions to the $3P_{3/2}$ state, and the A'-A'' doublet as transitions to the $3P_{5/2}$ states split into $3P_{5/2}(\Gamma_7^-)$ and $3P_{5/2}(\Gamma_8^-)$ by the cubic term. The $3P_{1/2}$ peak should occur at much higher energy and, like the $2P_{1/2}$ peak, is not easily resolved. Theoretical predictions for the $3P$ acceptor levels are not available at present, and the above interpretation is based on the strong similarity between the high-energy structure (attributed to $3P$ states) and the low-energy structure (attributed to $2P$ states). Before going on to the interpretation of acceptor spectra in other substances, we want to comment on the weak structure which is exhibited by the experimental spectra at an energy between that of line 1 and line 3. The theoretical

TABLE V. Energy of the acceptor states $2P_{3/2}(\Gamma_8^-)$ and $2P_{5/2}(\Gamma_8^-)$ for a few representative values of the coupling parameters μ and δ. The energies obtained by neglecting the second-order coupling produced by the cubic term between these states are compared with the more-accurate results that include such coupling. The energies are in units of the effective rydberg R_0.

	Without coupling		With coupling	
	$2P_{3/2}(\Gamma_8^-)$	$2P_{5/2}(\Gamma_8^-)$	$2P_{3/2}(\Gamma_8^-)$	$2P_{5/2}(\Gamma_8^-)$
$\mu=0.5$; $\delta=0.1$	0.468	0.333	0.473	0.331
$\mu=0.5$; $\delta=0.2$	0.468	0.357	0.490	0.346
$\mu=0.7$; $\delta=0.1$	0.767	0.502	0.778	0.498
$\mu=0.7$; $\delta=0.2$	0.767	0.552	0.820	0.531
$\mu=0.9$; $\delta=0.1$	2.268	1.564	2.436	1.508
$\mu=0.9$; $\delta=0.2$	2.268	2.079	3.454	1.758

TABLE VI. Energies of the lowest acceptor states which are not affected in first order by the cubic term. The energies are in units of the effective rydberg R_0.

μ	$1S_{3/2}$	$2S_{3/2}$	$2P_{1/2}$
0.00	1.000	0.250	0.250
0.05	1.002	0.251	0.238
0.10	1.009	0.254	0.227
0.15	1.021	0.258	0.217
0.20	1.037	0.264	0.208
0.25	1.060	0.273	0.200
0.30	1.089	0.284	0.192
0.35	1.125	0.297	0.185
0.40	1.171	0.313	0.179
0.45	1.228	0.333	0.172
0.50	1.299	0.358	0.167
0.55	1.388	0.388	0.161
0.60	1.503	0.426	0.156
0.65	1.653	0.476	0.152
0.70	1.857	0.542	0.147
0.75	2.145	0.635	0.143
0.80	2.580	0.773	0.139
0.85	3.309	1.003	0.135
0.90	4.768	1.460	0.132
0.95	9.145	2.820	0.128
1.00	∞	∞	0.125

predictions show that the only acceptor level in this energy range is that due to the $2S_{3/2}$ state, whose energy is given by line 2. The weak experimental structure always occurs at a slightly lower energy than line 2, and its energy position seems to depend on chemical effects. These facts confirm the interpretation that this structure is due to transitions from the ground state to the $2S_{3/2}$ excited state. In our effective-mass model both the initial and the final states of this transition belong to the Γ_8^+ irreducible representation of the group O_h, and an optical transition between them is strictly forbidden because the two states have the same parity.

The reason why this transition is experimentally observed may be found in our model potential for the acceptor center. We have assumed a screened Coulomb potential to describe the impurity, and since this potential has complete rotational symmetry, and is invariant under inversion through the origin, we have classified the acceptor states according to the irreducible representations of the group O_h. The actual symmetry around the impurity site is lower than O_h, and is given by the symmetry group T_d, [20] which does not contain the operation of inversion. The actual impurity potential in fact is not spherically symmetric, as we assume in our model, but belongs to the completely symmetric irreducible representation of the group T_d. This contradiction is the result of the fact that we have neglected central-cell effects. In fact, while at large distances from the impurity site the acceptor is well represented by a spherically symmetric potential, at small distances the impurity potential will have T_d symmetry because of crystal-field effects which are one of the reasons of the so-called central-cell corrections.

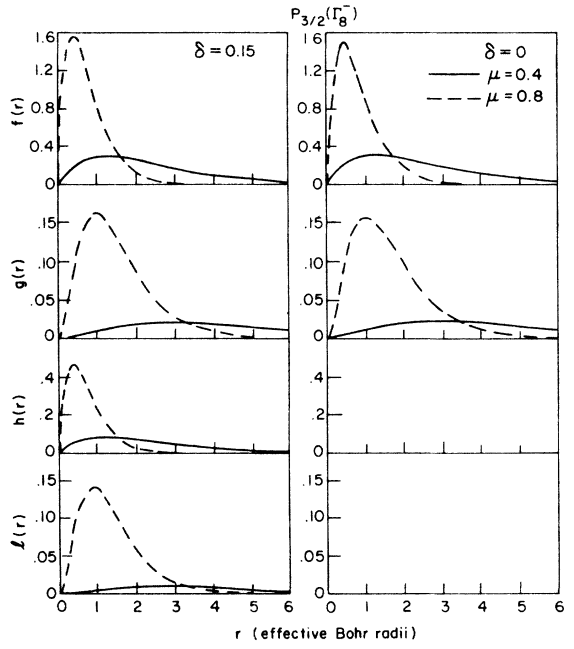

FIG. 5. Radial wave functions $f(r)$ and $g(r)$ for the acceptor state $2P_{3/2}(\Gamma_8^-)$ and for different values of μ and δ. The radial functions are normalized so that $\int_0^\infty [\,|f(r)|^2 + |g(r)|^2 + |h(r)|^2 + |l(r)|^2]\, r^2\, dr = 1$ and are given in units of $a_0^{-3/2}$, a_0 being the effective Bohr radius.

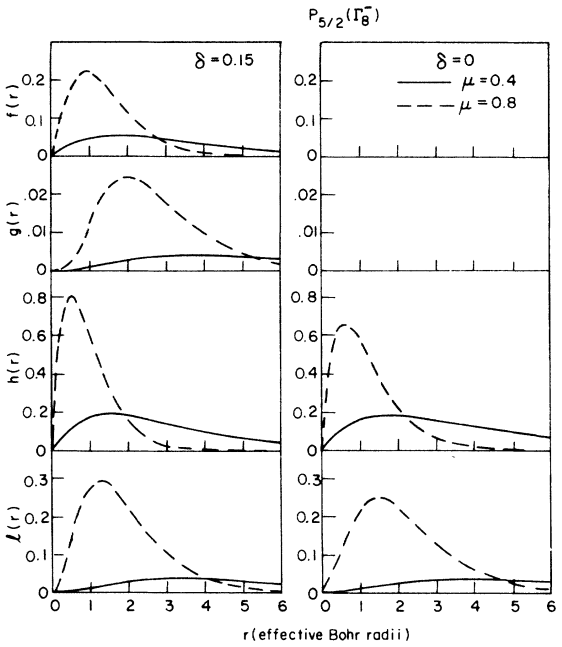

FIG. 6. Same as Fig. 5 but for the acceptor state $2P_{5/2}(\Gamma_8^-)$. The coupling with the acceptor states $P_{3/2}(\Gamma_8^-)$ is also shown.

The above argument proves why a weak optical transition from the ground state to the $2S_{3/2}$ state is experimentally observed. The energy position of the peak corresponding to this transition depends on the chemical species of the impurity. This is so because S wave functions have large amplitude near the origin, where the central-cell potential is particularly strong. We expect, however, a smaller chemical shift for the $2S_{3/2}$ state than for the $1S_{3/2}$ state, because in the latter state the impurity hole has a higher probability of being in the central cell. The experimental data provide the chemical shifts of the above states, and these are compared in Fig. 9. The straight line, which is a linear interpolation between the values for B and Tl impurities, shows that on the average the chemical shift of the $2S_{3/2}$ state is 7.1 times smaller than the shift of the $1S_{3/2}$ state. This value is in good agreement with the theoretical prediction given in our previous work[3]: that, for $\mu = 0.766$ (the parameter value

of Ge), the probability of being at the origin is 7.6 times smaller for $2S_{3/2}$ than for $1S_{3/2}$. The above ratios are not too different from the value of 8, which is expected for a simple hydrogenic model. This means that despite the complexity of the valence bands and the various splittings due to "spin-orbit" or cubic effects, the acceptor center still strongly resembles the simple hydrogenic model.

The excitation spectrum of acceptors and double acceptors in InSb has been studied experimentally by Kaplan.[18] Figure 10 shows the good agreement between the experimental data and our theoretical predictions. The striking feature of the experimental data is the strong similarity between the excitation spectra in InSb and those in Ge. Again the spectrum starts at low energy, with the weak peak due to transitions to the $2P_{3/2}$ state, and is dominated by the strong $2P_{5/2}$ doublet. Again the experimental data show the transition from the ground state to the $2S_{3/2}$ state, and clearly show that this transition is due to central-cell effects. In fact, the above transition is stronger in the case of silver impurities which have larger chemical shifts, as can be seen from the energy spacings of the lines.

An excitation spectrum completely similar to those in Ge and InSb has recently been observed by Stradling[19] for acceptors in GaAs. The agreement between theory and experiment is also excellent in this case. For example, the experimentally observed splitting of the $2P_{5/2}$ state is 2.0 meV, whereas our theoretical prediction is 1.9 meV, as can be obtained from Table VII.

Up to now we have considered only substances for which the cubic contribution is small, so that our perturbation treatment is valid. We have seen, that among the various diamond and zinc blende semiconductors considered in the present paper, only Si has such a large cubic term that perturbation theory is expected not to be valid.

TABLE VII. Theoretical energy spectrum of acceptor impurities in various semiconductors with the diamond and zinc blende structure. The parameters used in the calculation are given in Table I. The energy unit is meV.

	$1S_{3/2}(\Gamma_8^+)$	$2S_{3/2}(\Gamma_8^+)$	$2P_{1/2}(\Gamma_7^-)$	$2P_{3/2}(\Gamma_8^-)$	$2P_{5/2}(\Gamma_8^-)$	$2P_{5/2}(\Gamma_7^-)$
Si	31.56	8.65	4.18	12.13	8.51	5.86
Ge	9.73	2.89	0.61	4.30	2.71	2.04
AlSb	42.45	12.40	3.35	18.46	12.00	8.22
GaP	47.40	13.69	4.21	19.77	13.04	9.42
GaAs	25.67	7.63	1.60	11.38	7.20	5.33
GaSb	12.55	3.77	0.650	5.74	3.59	2.61
InP	35.20	10.53	1.97	15.89	9.98	7.32
InAs	16.31	5.00	0.420	7.91	4.76	3.63
InSb	8.55	2.63	0.155	4.24	2.54	1.91
ZnS	175.6	51.98	11.65	77.62	49.56	35.57
ZnSe	110.2	32.98	6.07	50.04	31.47	22.68
ZnTe	77.84	23.07	5.09	34.92	22.32	15.36
CdTe	87.26	26.42	3.70	41.43	25.85	17.68

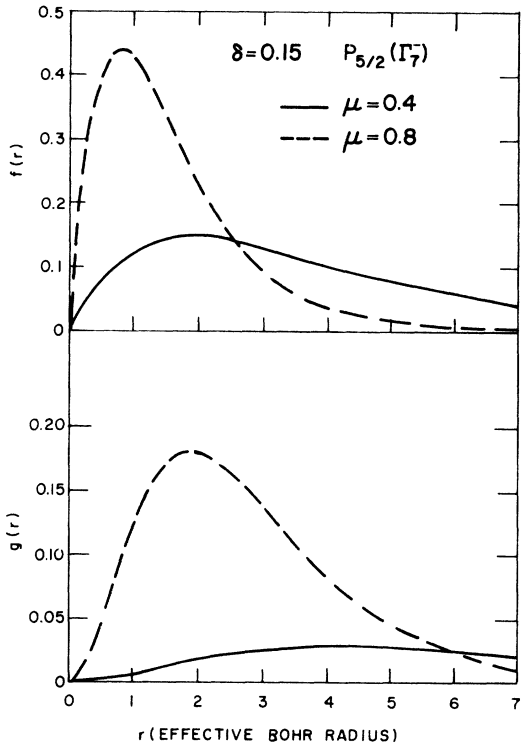

FIG. 7. Same as Fig. 6 but for the acceptor state $2P_{5/2}(\Gamma_7^-)$. The wave functions for $\mu=0.4$ and $\mu=0.8$ for $\delta=0$ are the same as those for $2P_{5/2}(\Gamma_8^-)$.

The differences introduced in the excitation spectrum by a large cubic term are immediately evident from a comparison of the spectra in Ge shown in Fig. 8 with those for the group-III acceptors in Si[16] given in Fig. 11. In the case of Si it has been impossible to obtain good agreement between the experimental data and the theoretical predictions. Nevertheless it is possible to give a tentative interpretation of the acceptor spectra in Si by using the experience gained from the interpretation of the spectra in Ge, InSb, and GaAs, and by using the theoretical energy spectrum in Si obtained with perturbation theory. As in the previous cases, the spectra start on the low-energy side, with the weak peak due to transitions to the $2P_{3/2}$ state (line 1 in Fig. 11). The $2P_{5/2}$ doublet is apparently missing from the spectra in Si. This is because the $2P_{5/2}$ state is split by the cubic term, which is particularly large in Si, and therefore the two partner lines of the doublet will be well separated in energy. Since we know that the doublet is the dominating feature in the excitation spectrum, we are tempted to interpret lines 2 and 4 as the partner lines of the doublet.

The interpretation of line 2 as being due to transitions to the $2P_{5/2}(\Gamma_8^-)$ state is confirmed by the theoretical prediction that this peak should be

3.6 meV at higher energy than the $2P_{3/2}$ peak or line 1 in Fig. 11. The assignment of line 4 as being due to transitions from the ground state to the $2P_{5/2}(\Gamma_7^-)$ state is less confirmed by theory, which predicts a $2P_{5/2}$ splitting of 3.6 meV compared to the experimental value of 5 meV. This discrepancy, however, is far from critical, since the above splitting is due to the cubic term, which has been considered in perturbation theory. Furthermore we notice that line 4 has a complicated structure. This seems to be in agreement with the previous assignment of the $2P_{5/2}(\Gamma_7^-)$ state and the fact that theory predicts a near degeneracy between $2P_{5/2}(\Gamma_7^-)$ and $2P_{1/2}(\Gamma_6^-)$. This is consistent with measurements under stress[16,21] for B impurities in Si, which suggest the participation of a Γ_6^- component in the complex line 4.

The position of the $2P_{1/2}$ peak is another difference between the acceptor spectra in Si and those in Ge, InSb, and GaAs, where the $2P_{1/2}$ state lies at very high energy, close to the series limit. A consequence of a large cubic term is that the hydrogenic $2P$ states have large splittings, and since they cover a wide energy range, they are expected to mix with the hydrogenic $3P$ states. An example of this is probably line 3, which measurements under stress[16,21] have shown to be due to transitions from the ground state to an excited state of symmetry Γ_8. Since the states with this symmetry and originating from the hydrogenic $2P$ state have been shown to be at lower energy, we tentatively interpret line 3 as due to transitions to the $3P_{3/2}$ state. A last remarkable feature in the excitation spectra of group-III acceptors in Si is their species dependence. We notice, for example, the absence of line 2 in the gallium spectrum and of line 3 in the aluminum spectrum. Both lines should occur at about 63 meV, and since this energy is close to that of the optical phonons in Si, it has been proposed[22] to explain their absence as being due to interaction with optical phonons. Furthermore, the acceptor spectra in Si show chemically dependent line spacings, in contrast to the case of Ge, and InSb, where the spacings are nearly constant. This high sensitivity to chemical shifts of the acceptor energy levels in Si is explained by the fact that, as shown in Table I, the acceptor Bohr radius in Si is 4 and 13 times smaller than those in Ge and in InSb, respectively. Since these crystals have nearly the same nearest-neighbor distance, this explains the larger sensitivity to chemical shifts that is found in Si.

V. CONCLUSIONS

We have studied the problem of shallow acceptor states in semiconductors taking into full account the band structure details for holes near the center of the Brillouin zone. Starting from the previously studied spherical model, we have included the effects of the generally small cubic

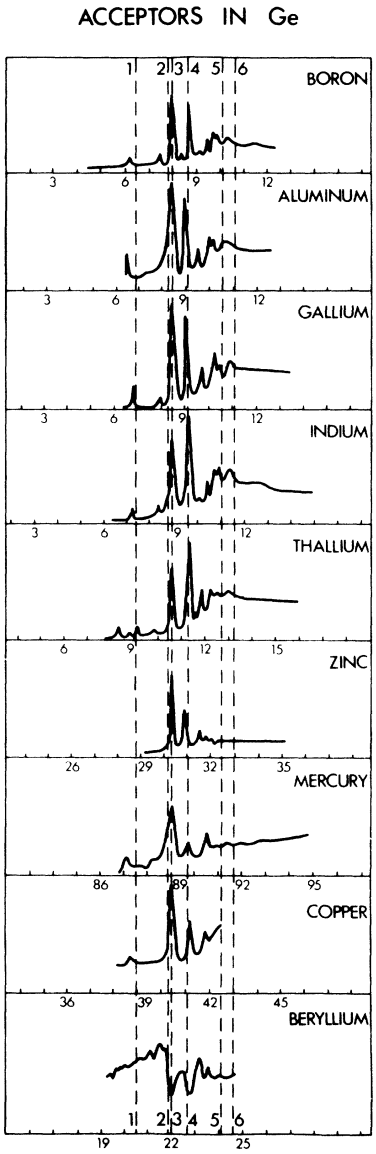

FIG. 8. Excitation spectra of various acceptors in germanium. The positions of the lines are accurate, but their intensities are only representative. The energy scales are the same for all impurities and have been shifted to bring into coincidence line 3. The vertical broken lines give the theoretical predictions ($1 = 2P_{3/2}$; $2 = 2S_{3/2}$; $3 = 2P_{5/2}(\Gamma_8^-)$; $4 = 2P_{5/2}(\Gamma_7^-)$; $5 = 2P_{1/2}$; $6 =$ series limit). Experimental data for group-III acceptors from Ref. 14; Zn from Ref. 21; Hg from R. A. Chapman and W. G. Hutchinson, Solid State Commun. 3, 293 (1956); Cu from P. Fisher and H. Y. Fan, Phys. Lett. 5, 195 (1960); Be from H. Shenker, E. M. Swiggard and W. J. Moore, Trans. Metall. Soc. AIME 239, 347 (1967).

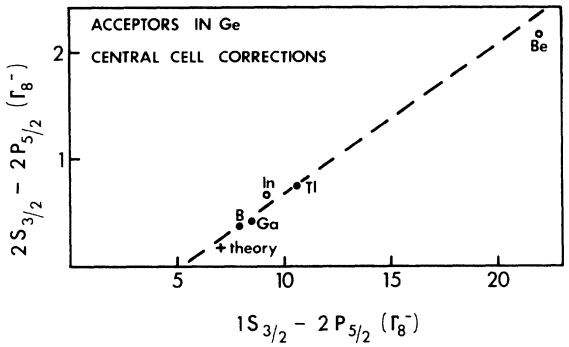

FIG. 9. Central-cell corrections of the states $1S_{3/2}$ and $2S_{3/2}$ for various acceptors in Ge. The open circles indicate that the experimental data is uncertain. The broken line is a linear interpolation between the data for B and Tl. The energies are in meV.

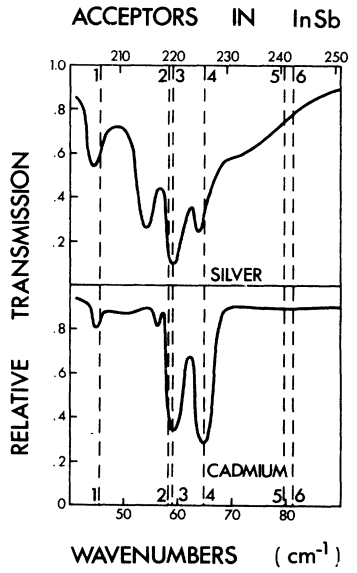

FIG. 10. Excitation spectra of silver and cadmium acceptors in InSb. See the caption to Fig. 8 for the explanation of symbols. The experimental data are from Ref. 18.

term that appears in the acceptor Hamiltonian. Since this term has been studied by using perturbation theory, the acceptor eigenvalues and eigenfunctions obtained in the present paper are valid only when the cubic perturbation is sufficiently small. We have shown that this condition is satisfied for most semiconductors with the diamond and zinc blende structure. The acceptor spectra in Ge, InSb, and GaAs have been interpreted both qualitatively and quantitatively. The acceptor spectra in other cubic semiconductors are expected to be very similar to those observed for the above substances, and their interpretation will not offer particular difficulties. The only exception among the semiconductors considered in the present paper is Si, which has completely different acceptor excitation spectra. This has been shown to be due to the anomalously large value that the cubic coupling parameter has for this crystal. Even in this extreme case, however, our perturbation treatment has allowed us to give a tentative qualitative interpretation of the experimental spectra. A quantitative interpretation of the spectra in Si has to wait for a treatment of the cubic term, which is more accurate than the present perturbation treatment.[23]

An important problem that is left unsolved in the present study is that of the species-dependent features which appear in the acceptor spectra in Ge, InSb, GaAs, and Si. For the reasons explained in Sec. IV, these effects are particularly important in the case of Si, where all acceptor levels seem to be species dependent. The solution of this problem requires a detailed study of the acceptor potential. In the present paper we have used a screened Coulomb potential and we have neglected short-range potentials which are due to the impurity core and which are responsible for the chemical shifts. Studies of the short-range component of the impurity potentials have been recently done by Baldereschi and Hopfield[24] in connection with the problem of isoelectronic traps, and by Pantelides and Sah[25] in connection with the problem of donor impurities in Si. Chemical shifts of acceptor states can be studied by following closely the above two works and by using the results of the present investigation. The spherically symmetric short-range potentials used up

TABLE VIII. Energy spacings of the excitation lines of various acceptor impurities in germanium. The theoretical values are also given and the energy unit is meV.

	Theory	B[a]	Al[a]	Ga[a]	In[a]	Te[a]	Zn[b]	Cd[b]	Hg[b]	Cu[b]	Be[b]
$2P_{5/2}(\Gamma_8^-)$-$2P_{3/2}$	−1.59	−1.70	−1.68	−1.70	−1.69	−1.70	−1.83	−1.68	−1.70	−1.72	−2.02
$2P_{5/2}(\Gamma_8^-)$-$2P_{5/2}(\Gamma_7^-)$	0.67	0.75	0.75	0.75	0.78	0.75	0.76	0.75	0.74	0.73	0.78
$2P_{5/2}(\Gamma_8^-)$-$2S_{3/2}$	−0.18	−0.37	···	−0.42	(−0.66)	−0.74	···	···	···	···	(−2.16)

[a]See Ref. 14.

[b]See Ref. 15.

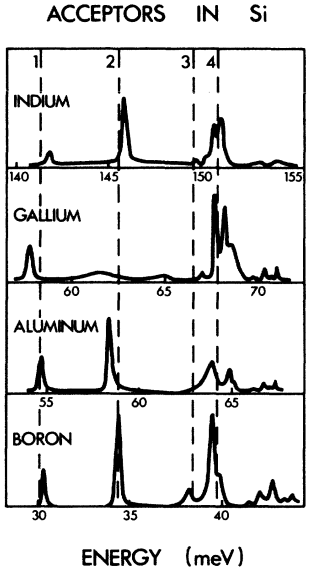

FIG. 11. Excitation spectra of group-III acceptors in silicon. The experimental data are from Ref. 16. The vertical lines in this case are not the theoretical prediction but an interpolation by hand on the experimental data. Line $1 = 2P_{3/2}$; $2 = 2P_{5/2}(\Gamma_8^-)$; $3 = 3P_{3/2}$; $4 = 2P_{5/2}(\Gamma_7^-)$ and $2P_{1/2}$.

to now, however, do not explain all the observed features of the acceptor spectra. As already mentioned, the observed optical transitions from the ground state to the excited $2S_{3/2}$ state cannot be explained in Si and Ge with a spherically symmetric central-cell potential. Probably crystal-field effects have also to be considered in the acceptor problem.

APPENDIX

In this Appendix we give the formulas which have been used to calculate the matrix elements of the cubic operator

$$Q = \alpha([P^{(2)}\times J^{(2)}]^4_4 + \tfrac{1}{5}\sqrt{70}\,[P^{(2)}\times J^{(2)}]^{(4)}_0 \times [P^{(2)}\times J^{(2)}]^{(4)}_{-4}) \quad , \tag{A1}$$

where α is a constant that assumes different values in the cases of strong and weak spin-orbit coupling, and the irreducible second-rank tensors $p^{(2)}$ and $J^{(2)}$ are derived from the Cartesian tensors (2a) and (2b), given in the text. The matrix elements of operator (A1) between states of given orbital angular momentum L, spin J and total angular momentum F (where $\vec{F} = \vec{L} + \vec{J}$), can be calculated by using the "reduced-matrix-element" technique, according to which the matrix elements are

$$\langle L', J', F', F'_z | [P^{(2)}\times J^{(2)}]^{(4)}_m | L, J, F, F_z\rangle = 3\times(-1)^{F'-F'_z}[(2F+1)(2F'+1)]^{1/2}\begin{pmatrix} F' & 4 & F \\ -F'_z & m & F_z\end{pmatrix} \times \begin{Bmatrix} J' & J & 2 \\ L' & L & 2 \\ F' & F & 4\end{Bmatrix} (L'\|P^{(2)}\|L)(J'\|J^{(2)}\|J) \quad . \tag{A2}$$

In the simpler case $F' = F$, expression (A2) reduces to formula (12), given in the text. For those interested in the derivation of (A2), we refer to the book by Edmonds.[12]

Expression (A2) reduces the evaluation of the matrix elements of the cubic operator to the calculation of 6-j symbols, 9-j symbols, and the reduced matrix elements $(L'\|P^{(2)}\|L)$ and $(J'\|J^{(2)}\|J)$. The expressions for the reduced matrix elements are explicitly given in the Appendix of our previous works,[3] since the same quantities were needed in the derivation of the spherical model. The values of the 6-j symbol have been tabulated by Rotemberg *et al.*[13] for low values of the angular momenta involved; all the values needed in the present work can be found there. The values of the 9-j symbols of interest have been calculated by the authors according to the expression given by Edmonds.[12] The values of the 9-j symbol used in the present work are the following:

(i) Cubic effect on $P_{5/2}$ states; Hamiltonians (14a) and (14b):

$$\begin{Bmatrix} \frac{3}{2} & \frac{3}{2} & 2 \\ 1 & 1 & 1 \\ \frac{5}{2} & \frac{5}{2} & 4\end{Bmatrix} = \tfrac{1}{150}\sqrt{15} \quad ,$$

$$\begin{Bmatrix} \frac{3}{2} & \frac{3}{2} & 2 \\ 3 & 3 & 2 \\ \frac{5}{2} & \frac{5}{2} & 4\end{Bmatrix} = \tfrac{-17}{29\,400}\sqrt{210} \quad ,$$

$$\begin{Bmatrix} \frac{3}{2} & \frac{3}{2} & 2 \\ 3 & 1 & 2 \\ \frac{5}{2} & \frac{5}{2} & 4\end{Bmatrix} = \begin{Bmatrix} \frac{3}{2} & \frac{3}{2} & 2 \\ 1 & 3 & 2 \\ \frac{5}{2} & \frac{5}{2} & 4\end{Bmatrix} = \tfrac{-1}{900}\sqrt{15} \quad ;$$

(ii) Cubic coupling between $P_{5/2}(\Gamma_8^-)$ and $P_{3/2}(\Gamma_8^-)$ states, Hamiltonian (15):

$$\begin{Bmatrix} \frac{3}{2} & \frac{3}{2} & 2 \\ 1 & 1 & 2 \\ \frac{3}{2} & \frac{5}{2} & 4\end{Bmatrix} = \tfrac{1}{300}\sqrt{30} \quad ,$$

$$\begin{Bmatrix} \frac{3}{2} & \frac{3}{2} & 2 \\ 3 & 3 & 2 \\ \frac{3}{2} & \frac{5}{2} & 4\end{Bmatrix} = \tfrac{11}{29400}\sqrt{70} \quad ,$$

$$\begin{Bmatrix} \frac{3}{2} & \frac{3}{2} & 2 \\ 1 & 3 & 2 \\ \frac{3}{2} & \frac{5}{2} & 4\end{Bmatrix} = \tfrac{3}{2100}\sqrt{30} \quad ,$$

$$\begin{Bmatrix} \frac{3}{2} & \frac{3}{2} & 2 \\ 3 & 1 & 2 \\ \frac{3}{2} & \frac{5}{2} & 4 \end{Bmatrix} = \frac{1}{1050}\sqrt{5} \quad ; \qquad \begin{Bmatrix} 1 & 1 & 2 \\ 3 & 3 & 2 \\ 2 & 2 & 4 \end{Bmatrix} = \sqrt{14}/3675 \quad ,$$

(iii) Cubic effect on P_2 states, Hamiltonians (18a) and (18b):

$$\begin{Bmatrix} 1 & 1 & 2 \\ 1 & 1 & 2 \\ 2 & 2 & 4 \end{Bmatrix} = \frac{1}{25} \quad , \qquad \begin{Bmatrix} 1 & 1 & 2 \\ 1 & 3 & 2 \\ 2 & 2 & 4 \end{Bmatrix} = \begin{Bmatrix} 1 & 1 & 2 \\ 3 & 1 & 2 \\ 2 & 2 & 4 \end{Bmatrix} = \frac{1}{525} \quad .$$

---

*Present address: Ecole polytechnique fédérale, Laboratoire de physique appliquée, Lausanne, Switzerland.

[1]N. O. Lipari and A. Baldereschi, Phys. Rev. Lett. 25, 1660 (1970).

[2]N. O. Lipari and A. Baldereschi, *Proceedings of the Eleventh International Conference on the Physics of Semiconductors* (Polish Scientific Publishers, Warsaw, 1972), Vol. 2, p. 1009.

[3]A. Baldereschi and N. O. Lipari, Phys. Rev. B 8, 2697 (1973).

[4]W. Kohn and D. Schecter, Phys. Rev. 99, 1903 (1955).

[5]D. Schecter, J. Phys. Chem. Solids 23, 237 (1962).

[6]K. S. Mendelson and H. M. James, J. Phys. Chem. Solids 25, 729 (1964).

[7]K. Suzuki, M. Okazaki, and H. Hasegawa, J. Phys. Soc. Japan 19, 930 (1964).

[8]V. I. Sheka and D. I. Sheka, Zh. Eksp. Teor. Fiz. 51, 1445 (1966) [Sov. Phys.-JETP 24, 975 (1967)].

[9]K. S. Mendelson and D. R. Schultz, Phys. Status Solidi 31, 59 (1969).

[10]J. M. Luttinger, Phys. Rev. 102, 1030 (1956).

[11]Throughout the paper the notation is that used by G. F. Koster, in *Solid State Physics*, edited by F. Seitz and D. Turbull (Academic, New York, 1957), Vol. 5.

[12]A. R. Edmonds, *Angular Momentum in Quantum Mechanics* (Princeton U. P., Princeton, N. J., 1960).

[13]M. Rotemberg, R. Bivins, N. Metropolis, and J. K. Wooten, *The 3-j and 6-j symbols* (Technical Press, Cambridge, Mass., 1959).

[14]For group-III acceptors in Ge, see R. L. Jones and P. Fisher, J. Phys. Chem. Solids 26, 1125 (1965).

[15]For group-II double acceptors in Ge, see W. J. Moore, J. Phys. Chem. Solids 32, 93 (1971).

[16]For group-III acceptors in Si, see A. Onton, P. Fisher, and A. K. Ramdas, Phys. Rev. 163, 686 (1967).

[17]A listing of experimental ionization energies is given in Table VI of Ref. 3. For the chemical effect on the ionization energies, see J. C. Phillips, *Bonds and Bands in Semiconductors* (Academic, New York, 1973) Chap. 9 (to be published).

[18]R. Kaplan, Solid State Commun. 12, 191 (1973).

[19]R. A. Stradling (private communication) (unpublished).

[20]See, for example, the review article by F. Bassani, in *Theory of Imperfect Crystalline Solids: Trieste Lectures* 1970 (IAEA, Vienna, 1971), p. 265.

[21]P. Fisher, R. L. Jones, A. Onton, and A. K. Ramdas, J. Phys. Soc. Japan Suppl. 21, 224 (1966).

[22]A. Onton, P. Fisher, and A. K. Ramdas, Phys. Rev. Lett. 19, 781 (1967).

[23]A more accurate treatment of the cubic term in the acceptor problem is presently under investigation. Preliminary results indicate that perturbation theory is quantitatively inadequate to treat the cubic term in the acceptor Hamiltonian of Si.

[24]A. Baldereschi and J. J. Hopfield, Phys. Rev. Lett. 28, 171 (1972); A. Baldereschi, J. Lumin. (unpublishe

[25]S. Pantelides and C. T. Sah, Solid State Commun. 1713 (1972); and unpublished.